Iranian Journal of Science & Technology, Transaction B, Vol. 28, No. B2
Printed in Islamic Republic of Iran, 2004
© Shiraz University

HYDROGEN DEGRADATION OF STEEL-DIFFUSION AND DETERIORATION*

M. FARZAM
Faculty of Petroleum Eng., Petroleum University of Technology, Ahwaz, I. R. of Iran
Email: farzam@put.ac.ir

Abstract – Permeation tests were conducted by Devanathan's electrochemical method and a newly invented electro-vacuum method. Experiments illustrated that as the microstructure changed, the diffusion constant, *D*, changed. The steel BS 4360 when quenched, decreased its *D* value by 3.7 times that of the original plate. Comparing the behavior of AISI 4340 with API X52, it is noted that the *D* value of the latter alloy is 2.23 times that of *API X*52, due to the presence of less *C* and Ni content. Ingress of hydrogen increased with the reduction of voltage and pH. For alloy BS 4360, when the charging voltage was dropped by -400 mv, the *D* value increased by 62%. Thickness would not have a realistic effect, but cold work reduced *D*. The same alloy when cold worked by 72%, its *D* value decreased by 15%. The difference in *D* measured by the two methods of permeation was due to the variation in material, apparatus design and operation.

Hydrogen degradation during stress corrosion and corrosion fatigue tests is one of the two processes of crack propogation. Immersion, dynamic polarization, stress corrosion (dynamic and static), corrosion fatigue tests, cathodic protection and fractographic studies were conducted in seawater and sour (hydrogen sulfide generated by sulfate reducing bacteria) environments. Overall, it was concluded that with regards to Nernest's equation, as the partial pressure of hydrogen increased, the value of *D* increased. Furthermore, the speed of hydrogen diffusion increased. In the sour environment, the overtaking mechanism of failure was found to be hydrogen embrittlement rather than anodic dissolution.

Keywords – Hydrogen degradation, diffusion, diffusion constant, fatigue, corrosion, stress corrosion, cracking

1. INTRODUCTION

Following aqueous surface electrochemical reactions and hydrogen reduction, atomic hydrogen will diffuse through steel to reside at the microstructural defects with possible catastrophic failures to follow. Carbon steel, low alloy steel or high strength low alloy steel under no-load, static or cyclic loading will be affected by the presence of hydrogen. Such an effect is mainly influenced by temperature, alloying, residual and applied stress, and partial pressure of hydrogen.

The sources of hydrogen production in the industry are many Eqs. (1-3)

Water dissociation $H_2O \longrightarrow H^+ + OH^-$ (1)

Fe–H_2O reaction $2Fe + 3H_2O \longrightarrow Fe_2O_3 + 3H_2$ (2)
$(H + H \Leftrightarrow H_2)$

Effect of pH and bacteria $H^+ + e \longrightarrow H$ (3)

Following atomic hydrogen production at the cathodic side of a corrosion cell, hydrogen will diffuse into steel residing at the lattice interstitial sites, grain boundaries, vacancies, impurities and alloying elements. The bonding energy of such interactions are different, trap sites are either low energy reversible (e.g. interstital solutes 3-15 KJ/mol [1]) or high energy irreversible (e.g. TiC particles 96 KJ/mol [1]).

*Received by the editors February 16, 2002 and in final revised form November 30, 2003

Archive of SID
www.SID.ir

It is believed that steel with high energy traps will release hydrogen at higher temperatures (about or higher than 250^0C). Generally hydrogen will not saturate, and therefore is less likely to damage the austenitic stainless steels, but carbon steel and ferritic or martensitic steels will be degraded and finally cracked. Hydrogen degradation will appear in one of the following forms [16]: 1) Hydrogen embrittlement, 2) Hydrogen blistering, 3) Hydrogen induced cracking.

As little as H<1 ppm is enough to damage steel.

There are a number of theories describing the mechanisms of H degradation [16]: 1) Pressure theory, 2) Surface energy, 3) Enhanced plastic flow, 4) Transport model, 5) Hydride formation, 6) Decohesion theory

Since the diffusion of hydrogen into austenitic stainless steel will not increase the internal gas pressure, the pressure theory cannot be generally applicable. As far as the surface energy theory is concerned, as the oxygen absorption at the surface will not reduce the surface energy (with higher absorption energy than H), this theory may also not always be applicable. The third theory, which discusses the enhancement of plastic deformation in the presence of H, has rarely been approved and reported. The fourth theory describes the hydrogen transportation by dislocations, but in the absence of dislocations, hydrogen will also diffuse and be transported. There is an interaction of hydrogen with alloys such as Nb, e.g. *Nb-H*, which is a brittle compound (the fifth theory). Such an effect cannot also be a prime factor of degradation.

It is generally believed that the last theory (number six), the decohesion theory, is the major responsible factor for weakening the Fe-Fe bonds, and that a hydrogen failure is the result of the participation of all six theories.

The temperature at which hydrogen will inflict its severest damage is at about 25^oC [2]. Figure 1 shows that the crack advance at this temperature is maximum. The figure also shows that the higher the steel's strength, the faster the crack propagation rate. The effect of hydrogen when coupled with static and cyclic stresses will be reflected as stress corrosion, corrosion fatigue or a combination of the two, i.e. stress corrosion fatigue [3, 4].

The hydrogen diffusion characteristics previously reported by Devanathan and Stachurski [5] (Fig.2) showed that it takes an incubation period, t_b, before hydrogen reaches the exit surface. The amount of hydrogen reaching the exit side increases and reaches a steady-state with time. Time t_b and the area under the curve is representative of the metal's characteristics.

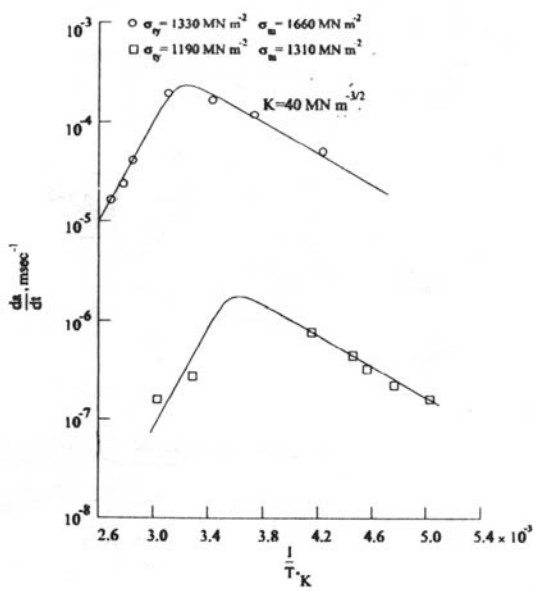

Fig. 1. Crack advance Vs temperature in AISI 4130 [2]

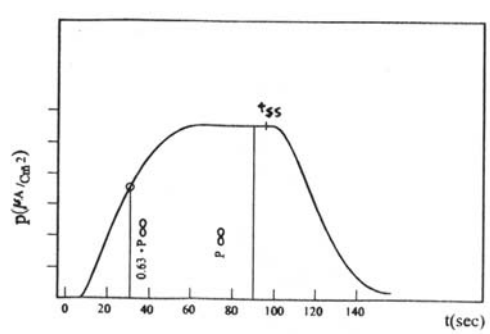

Fig. 2. Hydrogen diffusion curve [5]

Hydrogen diffusion obeys Fick's first law

www.SID.ir

$$J=-D\frac{dc}{dx} \tag{4}$$

where J is the flux in $mol/cm^2\,S$, D is the diffusion constant in cm^2/S, C is the concentration in mol/cm^3 and X is the distance hydrogen travels in cm.

$$D=D_0 exp\frac{-Q}{RT} \tag{5}$$

where D is a constant, Q is the activation energy in J/mol, R is the gas constant in $J/mol\ K$ and T is the temperature in K.

It has been shown experimentally that

$$D=\frac{L^2}{6t_{lag}} \tag{6}$$

where L is the thickness in cm and t_{lag}= 0.63 J steady-state. From Fig. 2, t_{lag} is measured at the intersection of the vertical line with the tangent of the slope at $0.63P_{S.S}$. Some researchers [6] have used the $0.83_{S.S}$. Devanathan and colleagues [5] showed that as the voltage decreased, the amount of hydrogen diffused increased and D was not a function of thickness. Detailed research has been conducted on the effect of microstructure on hydrogen diffusion [7]. The concluding remarks on such an effect are that the structural inhomogeneities; line defects, impurities (TiC) or martensitic laths, will trap hydrogen and degrade the microstructure. The lower the hydrogen-defect bonding energy and the less such microstructure inhomogeneities, the less the amount of trapped hydrogen and the less likelihood of hydrogen degradation. Other researchers have reported their findings on the increase of the number of dislocations and therefore the amount of trapped hydrogen and trapping energies [8, 9]. Their conclusions include that having a homogeneous structure reduces the risk of hydrogen damage. Variation of D with microstructure and alloying is definite, and it may be stated that the lower the D, the lower the amount of diffused hydrogen [10]. Therefore, if the amount of trapped hydrogen is lowered, the possibility of hydrogen damage is decreased. It may be suggested that by controlling the microstructure, hydrogen degradation is controlled. Considerable research has been previously conducted on the fractography of fractured surfaces. In a stress corrosion cracking study in H_2S, Huang and Shaw [11] showed that the crack morphology was quasi-brittle and the observed white markings were considered a sign of the presence of hydrogen. As it will be noticed below, almost all findings reported above are reaffirmed in this work and this author accept them.

2. EXPERIMENTAL PROCEDURE

Diffusion measurements have been either conducted by an electrochemical [5] or a dry gas technique [8]. In the electrochemical method a steel sample is situated between an anodic cell and a cathodic charging cell. When a potential difference between the two sides is established due to the presence on the cathodic side, H diffusion takes place and after a while is detected at the anodic side. Hydrogen diffusion increases with time, reaching a maximum of a steady-state amount. As with the decrease in negative charging potential, the $P_{s.s}$ is increased (Nernest Eq.) (See discussion, Eq. (7)).

This article represents more than twenty years of intense and continuous research, beginning at Sheffield University (U.K.), then at Heriot-Watt University (U.K.), and afterwards in Iran. The electrochemical technique was used at Sheffield, while a newly invented method by this author, which is a cross technique between the electrochemical and vacuum (gaseous) techniques was employed at Heriot-watt (Scotland, U.K.). The results were then correlated with stress corrosion, corrosion fatigue, and case studies in Iran [16]. Figures 3 and 4 show the apparatus used in the present investigation.

Archive of SID

www.SID.ir

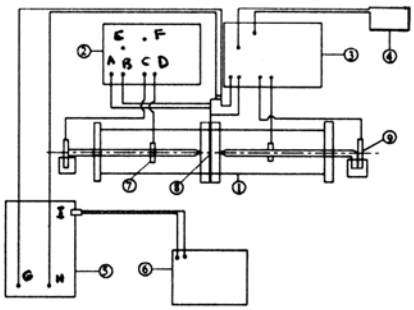

LIST	
Compenent	Description
1	The Cell
2	Potentiostat, Charging
3	Potentiostat, Detecting
4	Digital Meter (A,V)
5	Electrometer (Vibran)
6	Recorder
7	Auxilliery Electrode
8	Speciman
9	Reference Electrode
INSTRUMENTAL DESIGNATION	
Representation	Function
A	Working Electrode
B	Remote Sensing
C	Reference Electrode
D	Auxilliary Electrode
E	Common
F	Internal Reference (Nessuro)
G	Low
H	High
I	Out put

Fig. 3. Devanathan cell construction used for electrochemical testing [8]

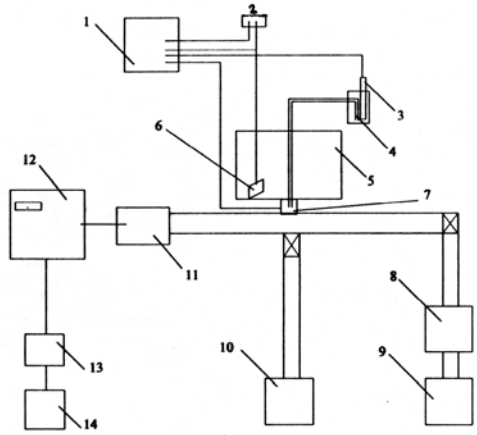

1 - Potentiostat
2 - Digital ammeter
3 - Reference electrode
4 - Salt bridge
5 - Corrosion cell
6 - Platinum auxiliary electrode
7 - Test sample
8 - Diffusion pump
9 - Rotary pump
10 - Ion pump
11 - Mass detector
12 - Intelligent mass spectrometer
13 - Computer
14 - Printer

Fig. 4. Apparatus used for electro-vacuum testing

www.SID.ir

The electro-vacuum testing technique used a cathodic electrochemical cell to charge the hydrogen into steel, and a vacuum (10^{-7} torr) side leading to a mass-spectrometer to detect the amount of hydrogen diffused through, using a computer. Table 1 gives details of the alloying elements of the steels tested by the electrochemical method. The API 5LX65 was used to transport liquid gas. Hydrogen-induced cracking was observed in this steel during service, (as was reported by British Gas) and cracking occurred at positions where the microstructure due to the segregation of *Mn* (*Mn*=2%), was martensitic. The steel's structure was similar to BS 4360 (Table 1). There are a few reasons why the alloy used in this paper are in accordance with different standards. Firstly because this work covers more than 20 years research on hydrogen diffusion and degradation phenomena, secondly each metal supplied in different stages was purpose (tailor) made for a specific application. However the reader is kindly referred to Ref. [17] for AISI/ SAE 4340 page 70, for BS 4360 page 202 and for *API X*65 page 332.

Table 1. Analysis of steels used for hydrogen permeation test (Devanathan)

Material	C	Mn	Si	S	P	Cr	Ni
API X65(Low S)	0.079	1.33	0.29	0.004	0.006	-	-
API X65(High S)	0.089	1.38	0.31	0.031	0.005	-	-
BS 4360	0.13	1.57	0.32	0.007	0.008	0.11	0.15
BS 4360 (Quenched)	0.13	2.23	0.31	0.01	0.008	-	-

The steel samples were Pd-plated and tested in caustic soda (0.1N NaOH) at potentials lower than –1300 mv. During these tests, the effects of thickness, voltage and plastic deformation (after 72% R.A.) on variation in *D* were recorded. Table 2 shows some of the results obtained. Please note that not all reference electrodes used were Calomel electrodes ($Hg, Hg_2Cl_2/Cl^-$).

Table 2. Results of Devanathan test (0.1 NaOH, 2mm thick)

Material	t_{lag}(min)	D(cm^2/ S $\times 10^{-6}$)
API X65(Low S)	68.75	1.61
API X65(High S)	77.5	1.43
BS 4360	69	1.61
BS 4360 (Quenched)	253	0.44

Table 3. Steel analysis used for hydrogen permeation test (Electro-Vacuum)

Material	C	Mn	Si	S	P	Cr	Ni
APIX-52	0.14	1.33	0.33	0.003	0.008	0.05	0.03
AISI 4340	0.38	0.73	0.2	0.016	0.13	1.08	1.38

Table 3 gives details of the alloys tested by the electro-vacuum method. API 5LX52 steel may also be used to carry liquid gas or other petroleum products, and AISI 4340 is used as a well casing material. Table 4 shows the results obtained in 0.1N NaOH for these latter two steels.

For the reason of an actual simulation, the steel samples were not plated in the latter tests. During these tests, the effects of environmental change, thickness and voltage were examined (see Table 5). The inhibitor used was supplied by the Chevron Company and was organic amine based. Two cases of fractured surfaces were compared with one another to find footprints of hydrogen:

1. A case of stress corrosion fatigue of high strength steel cables that failed in H_2S environment,
2. Another case of stress corrosion fatigue of N.I.O.C drill pipes [15].

It is worth mentioning that other stress corrosion and corrosion fatigue tests were conducted that are not all stated here. The stress corrosion tests were conducted either statically (80%S_{yield}) or dynamically (slow strain rate=$10^{-5}S^{-1}$). The corrosion fatigue tests were conducted at 0.167 Hz frequency and constant stress range. These latter tests were conducted on AISI 1055, 1075, and 50B60 in putrid seawater (H_2S = 200 ppm) [14]. As the emphasis here is on the kinetics of hydrogen diffusion rather than on fracture morphology, only a few fractographs are presented in this paper. Some of the linear polarization, potential and pH measurements conducted on the cables show the rate and possible change in the types of reactions. Immersion tests were also conducted in the sour environment.

Archive of SID

www.SID.ir

Table 4. Results of electro-vacuum test (0.1N NaOH, 2mm thick)

Material	t_{lag}(min)	D(cm^2/S $\times 10^{-7}$)
API X52	242	4.58
AISI 4340	541	2.05

Table 5. Results of Electro-Vacuum test (0.5 mm)

Material	Environment	t_{lag}(min)	D(cm^2/S $\times 10^{-7}$)
AISI 4340	0.1 N NaOH	82	0.84
AISI 4340	Seawater	62	1.12
AISI 4340	Seawater +	56	1.24
API X52	Inh.	90	0.77
API X52	0.1 N NaOH	62	1.12
API X52	Seawater	28	2.48
API X52	H_2S	42.5	1.63
	H_2S + Inh.		

Inh : Inhibitor
H_2S : Seawater + H_2S

3. RESULTS AND DISCUSSION

Diffusion tests conducted by Devanthan's electrochemical method (Table 2) showed that with the increase in sulphur *X*65, *D*, the diffusion coefficient decreased from 1.61×10^{-6} to 1.43×10^{-6} cm^2 /S. This was due to the increased MnS surface area. MnS would act as a trap impeding hydrogen transport. The measured D for BS 4360 was similar in value to that for *X*65, and was equal to 1.61×10^{-6} cm^2/S.

Alloy BS 4360 with higher Mn when quenched, showed an increased t_{lag} and a decreased D of 0.44×10^{-6} cm^2 /S (Table 2). This result was attributed to the presence of fine laths of martensite, which is saturated in carbon and is an internally stressed structure (shear-induced transformation). Figure 5 compares the behaviors of *X*65 and the quenched 4360. The figure shows 4360 to have the longer t_b.

Recharging the test sample (second transient) after the first transient produced a shorter t_b and increased D. This was ascribed to the saturation of the traps during the first transient. Lowering the steady-state flux was a sign of reduction in *dc/dx* according to Fick's first law. However, this may change (i.e. increase the steady-state) for a different alloying element. When BS 4360 was cold worked (72% reduction in area, 0.5 mm thickness), t_b increased from 6 to 112 min, and *D* decreased from 4.62×10^{-6} to 5.3×10^{-7} cm^2 /S. This was due to increased dislocation density (10^6 to 10^{12} cm/cm^3) acting as strong traps. Vicker's hardness showed an increase from 183 to 272 HV. This fact may be related to the increased dislocation density.

When the charging voltage was decreased from -1300 to -1700 mv, *D* increased from 4.3×10^{-6} to 6.9 *X* 10^{-6} cm^2 /S, this may be explained according to the Nernest's equation (increase in hydrogen partial pressure).

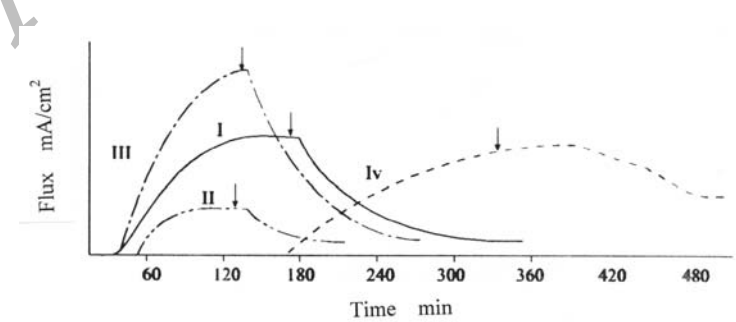

Fig. 5. Hydrogen diffusion measurements conducted by Devanathan's method (2mm thick) (I) X-65(low S); (II) X-65 (high S); (III) BS 4360; (IV) BS 4360 (quenched)

Nernest's Eq. $$-E = -E_o + RT/ZF \; Ln\, P_{H2} - \text{constant}\, pH \quad (7)$$

As the thickness was decreased from 2 to 0.5 mm, *D* increased from 1.6×10^{-6} to 4.3×10^{-6} cm^2/S. This change was only due to the kinetics of the electrode's surface. The electro-vacuum tests conducted on API *X*52 and AISI 4340 (Fig. 6) were made without Pd coating of the test samples.

Archive of SID

www.SID.ir

Published research has shown that the volume of hydrogen diffusing through would increase with the increase in surface scratches as a result of the increase in surface area [12]. Thus, during the present series of tests, all the samples were polished with 600 grade SiC paper and used uncoated. Other investigators reported unsuccessful test results if the samples were not Pd-coated [13]. In the present work, the measured D for *X*52 was twice that of 4340. A comparison of the alloying elements of the two metals indicates that AISI 4340 has a higher amount of *C*, *Cr*, *Ni* and *S*. It is generally believed that elements on the right-hand side of Fe in the periodic table (*C*, *Ni*, etc.) repel hydrogen, while elements on the left- hand side of Fe (*Cr*, *Ni*, etc.) attract hydrogen. A comparison of *D* values for the electro-vacuum tests with those of the electrochemical experiments reveals that *D* was 10 times larger (faster) for the electrochemical tests. This is most likely due to the surface impedance of the scales (absence of Pd), in addition to variations resulting from the electro-vacuum test method. Table 5 shows that *D* changed with the changes in the test environment. Testing AISI 4340 in 0.1N NaOH provided $D = 0.84\times10^{-7}$ cm^2/S, which is similar to that for API X52. But when *X*52 was tested in H_2S, *X*52, *D* increased from 0.77 to 2.48×10^{-7} cm^2/S, linear polarization tests conducted in H_2S on AISI 1074 showed that FeS resulted in cathodic depolarization (see Fig. 7). Thus, with the increase in cathodic reaction, the amount of hydrogen reduction and diffusion would increase. This matches the results obtained during diffusion (Table 5).

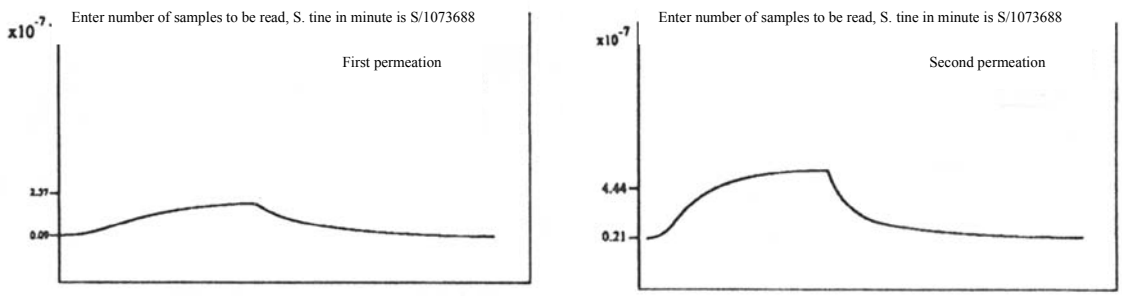

Fig. 6. Hydrogen diffusion measurements by the electro-vacuum testing technique

The free corrosion potential of steel in the presence of H_2S will change with time. Figure 10 shows that with time (after 219 h) the potential of AISI 1055 increased from -720 to –560 mv. This may be due to the change in FeS stoichiometry, perhaps to FeS_2. When the corroded surface was cleaned it was noted that pits had formed under the black FeS layer (see Fig. 9).

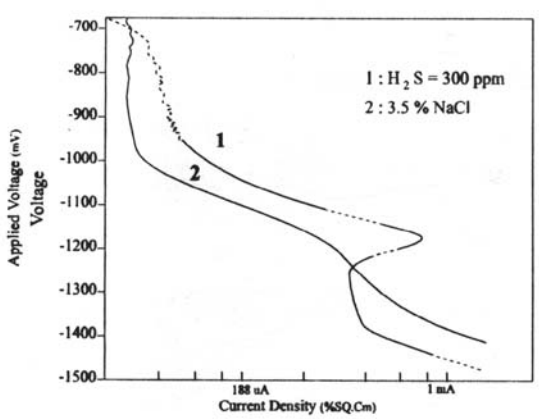

Fig. 7. Linear polarization (cathodic side) in: (1) seawater+ H_2S = 300 ppm; and (2) 3.5% NaCl solution

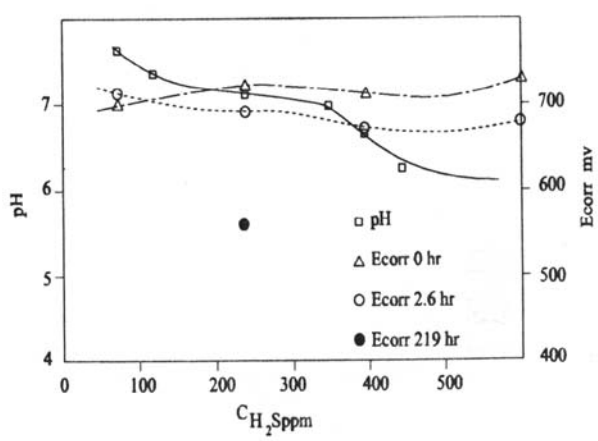

Fig. 8. Changes in E_{corr} in different H_2S concentrations for AISI 1055

Corrosion fatigue and stress corrosion tests were conducted on wires and wire-ropes (AISI 1055, 1074, and 50B60) in an H_2S environment. In the fatigue tests, the number of cycles to failure decreased as the maximum stress increased. This was considered as a sign of stress corrosion fatigue failure. Cracks were noted to originate from the corrosion-pits formed under perforated FeS layer (Fig. 10). Thus, one can say

www.SID.ir

that the crack initiation mechanism is anodic dissolution. White marking, as a result of hydrogen embrittlement was observed on the fractured surface (Fig. 11), also refer to reference No. 11. Thus, hydrogen embrittlemnt could be the mechanism of crack propagation.

Fig. 9. Pitting corrosion of AISI 1055 in H_2S

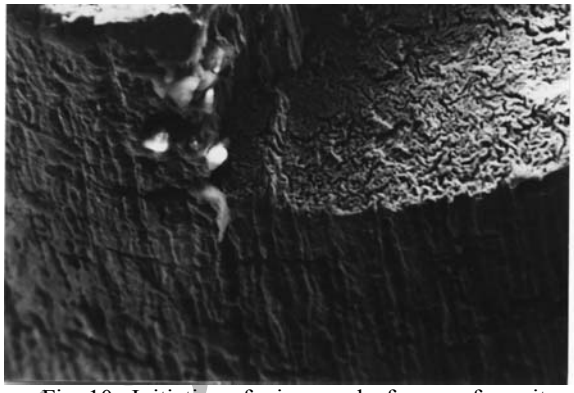

Fig. 10. Initiation of microcracks from surface pits (anodic dissolution)

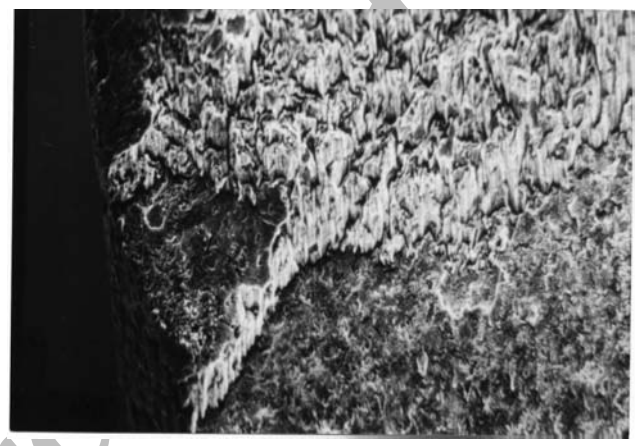

Fig. 11. Signs of hydrogen embrittlement (white markings)

Drill pipe failure (NIOC) showed that in the alkaline environment of the drill mud (pH=10), fracture was due to a combination of tensile and torsional cyclic stress. The fractured surface showed a thumbnail fatigue fracture with surface scratches and micro-cracks acting as the initiating sites. Thus, the initiation and propagation mechanisms seem to be via anodic dissolution. However, the presence of cyclic loading may imply a stress corrosion fatigue failure [15].

4. CONCLUSIONS

1. With an increase in sulphur, t_{lag} increased.
2. Quenched BS 4360 had a *D* four times slower than pearlitic structure.
3. D measured by the electro-vacuum method was ten times that by Devanathan.
4. In the presence of H_2S, *D* increased.
5. In the presence of inhibitors, *D* did not decrease.
6. Reduction in voltage increased *D*.
7. The lower the value of *D*, the less susceptibility to hydrogen degradation.
8. The alloying elements will effect *D*.
9. Cold reduction will decrease *D*.
10. Stoichiometry of corrosion products affects the diffusion rate.
11. H_2S increases stress corrosion fatigue susceptibility.
12. Fracture surface reveals environments effect: as white markings were related to hydrogen degradation.

www.SID.ir

13. NIOC drill pipe failure in drill mud followed anodic dissolution mode, both at initiation and propagation stages.
14. Wire rope failures in H_2S environment showed anodic dissolution mode at the initiation stage and hydrogen embrittlement assisted fracture at the propagation stage.
15. The fracture type in the presense of H_2S was a quasi- brittle one.

REFERENCES

1. Gibala, R. & Kumnick, A. J. (1984). *Hydrogen trapping in iron and steels, in: Hydrogen embrittlement and stress corrosion cracking*. Ed., R. Gibala and R. F. Hehemann, ASM, 61.
2. Johnson, H. H. (1984). *Overview on hydrogen degradation phenomena, in: Hydrogen embrittlemnent and stress corrosion cracking*. Ed., R. Gibala and R. F. Hehemann, ASM, 3.
3. Ford, F. P. (1982). *Stress corrosion cracking, in corrosion processes*. Ed., R. N. Parkins, Applied Science Publishers, 271.
4. Congleton, J. & Craig, I. H. (1982). Corrosion Fatigue. Applied Science Publishers, 209.
5. Devanathan, M. A. V. & Stachurski, Z. (1964). Mechanism of hydrogen evolution on iron in acid solutions by determination of permeation rates. *Journal of the Electrochemical Society*.
6. McBreen, J., Naris, L. & Beck, W. (1966). A method for determination of the permeation of hydrogen through metal membranes. *Journal of the Electrochemical Society*, *Nov*., 1220.
7. Bernstein, I. M. & Thompson, A. W. (1984). *The role of microstructure in hydrogen embrittlement: in Hyrogen embrittlement and stress corrosion cracking*. Ed., R. Gibala and R. F. Hehemann, ASM a book, 135.
8. Johnson, H. H. & Way Lin, R. (1984). *Hydrogen and deuterium in iron, in: Hydrogen effects in metal*. Ed., I.M. Bernstein and A.W. Thompson, ASM, 3.
9. Kim, K. K. & Pyon, S. (1988). Hydrogen permeation through 3.3% Ni-1.6% Cr steel during plastic deformation. *Scripta Metallurgica, 22*, 1719.
10. Tseng, C. H., Wei, W. Y. & Wu, J. K. (1989). Electrochemical methods for studying hydrogen diffusivity, permeability in AISI 420 and 430 stainless steels, *Materials Science and Technology, 5*, 1236.
11. Huang, H. & Shaw, W. J. D. (1993). Cold work effects on sulphide stress cracking of pipeline steel exposed to sour environment. *Corrosion Science, 34*(1), 61.
12. Reuben, R. L. (1980). Hydrogen permeation. Ph.D. Thesis, Open University, U.K.
13. Bernstein, I. M. & Thompson, A. W. (1978). Proc. Mechanisms of Environmental Embrittlement in Materials Metal Society, 403.
14. Farzam, M., Brook, R. & Edyvean, R. G. J. (1990). The fracture of steel wire, strand and rope in marine environments. *31st Corrosion Science Symposium, 11-14 Sept*., Newcastle, England.
15. Ghasemi, P. & Baigi, M. M. (1995). B.Sc. graduate project under Dr. M. Farzam Supervision, PUT, Ahwaz, Iran.
16. Farzam, M. (2000). *Corrosion engineering and protection*. Book, Yadvareh Ketab Publishers, 64-72.
17. British steel Corporation (1979). *Iron and steel specification*. Publication No. X005.5M. 11.79 5th Edition, P70, P202, P332.

Archive of SID

www.SID.ir